



IMMUNOPATHOLOGY AND INFECTIOUS DISEASES

# Compartmentalization of Immune Responses during *Staphylococcus aureus* Cranial Bone Flap Infection

Joseph Cheatle,\* Amy Aldrich,† William E. Thorell,\* Michael D. Boska,‡ and Tammy Kielian†

From the Division of Neurosurgery,\* Department of Surgery, and the Departments of Pathology and Microbiology,† and Radiology,‡ University of Nebraska Medical Center, Omaha, Nebraska

Accepted for publication  
April 25, 2013.

Address correspondence to  
Tammy Kielian, Ph.D., Department of Pathology and Microbiology, University of Nebraska Medical Center, 985900 Nebraska Medical Center, Omaha, NE 68198-5900.  
E-mail: tkielian@unmc.edu.

Decompressive craniectomy is often required after head trauma, stroke, or cranial bleeding to control subsequent brain swelling and prevent death. The infection rate after cranial bone flap replacement ranges from 0.8% to 15%, with an alarming frequency caused by methicillin-resistant *Staphylococcus aureus*, which is problematic because of recalcitrance to antibiotic therapy. Herein we report the establishment of a novel mouse model of *S. aureus* cranial bone flap infection that mimics several aspects of human disease. Bacteria colonized bone flaps for up to 4 months after infection, as revealed by scanning electron microscopy and quantitative culture, demonstrating the chronicity of the model. Analysis of a human cranial bone flap with confirmed *S. aureus* infection by scanning electron microscopy revealed similar structural attributes as the mouse model, demonstrating that it closely parallels structural facets of human disease. Inflammatory indices were most pronounced within the subcutaneous galeal compartment compared with the underlying brain parenchyma. Specifically, neutrophil influx and chemokine expression (CXCL2 and CCL5) were markedly elevated in the galea, which demonstrated substantial edema on magnetic resonance images, whereas the underlying brain parenchyma exhibited minimal involvement. Evaluation of immune mechanisms required for bacterial containment and inflammation revealed critical roles for MyD88-dependent signaling and neutrophils. This novel mouse model of cranial bone flap infection can be used to identify key immunologic and therapeutic mechanisms relevant to persistent bone flap infection in humans. (*Am J Pathol* 2013, 183: 450–458; <http://dx.doi.org/10.1016/j.ajpath.2013.04.031>)

Decompressive craniectomy is performed after head trauma, stroke, or cranial bleeding, where a portion of the skull is removed to control subsequent brain swelling and prevent death. After removal, the bone flap is often cryopreserved until replacement; however, this increases the likelihood of destroying its blood supply, which substantially augments risk of infection.<sup>1</sup> The prevalence of infection after craniotomy ranges from 0.8% to 15%, with an alarming frequency caused by methicillin-resistant *Staphylococcus aureus* (MRSA), a major community and nosocomial gram-positive pathogen.<sup>2</sup> This high infection rate subjects patients to at least two additional surgical procedures since it is not possible to clear the infected bone *in situ* because of its recalcitrance to antibiotic therapy.<sup>3</sup> In the first procedure, the infected skull flap is removed, and after a variable period of antibiotic therapy ranging from 6 weeks to >12 months, a second procedure is performed to place an expensive custom

alloplastic flap composed of either acrylic resins, titanium mesh, or hydroxyapatite.<sup>3,4</sup> In approximately 13% of patients, prolonged absence of the skull flap can lead to syndrome of the trephined, a series of adverse effects that can include headache, seizures, mood swings, and behavioral disturbances.<sup>5–7</sup> Treatment of trephine syndrome consists of replacement of the original bone flap or synthetic device<sup>8,9</sup>; however, this cannot be performed until there is convincing evidence that any residual infection associated with the original bone/artificial flap has been eliminated.

Currently, cranial bone flap infections cannot be prevented or effectively treated without removal of the infected

Supported by the NIH, National Institute of Allergy and Infectious Disease, P01 AI083211 Project 4 (T.K.), and the University of Nebraska Medical Center, Division of Neurosurgery (W.E.T.).

J.C. and A.A. contributed equally to this work.

flap, and little information is available about the immune or microbial attributes that contribute to disease chronicity. These are important issues because a better appreciation of key pathogenic factors may reveal new targets to prevent and/or treat bone flap infections. Here we report a novel mouse model of *S. aureus* cranial bone flap infection that accurately mimics several facets of human disease in response to a relatively low infectious inoculum. This model has revealed that distinct immune responses are elicited within the subcutaneous space and brain parenchyma even though both bone flap surfaces communicate with these compartments and harbor similar numbers of bacteria. This information will help to facilitate the future design of novel therapeutic targets to prevent and/or treat bacterial cranial bone flap infections.

## Materials and Methods

### Mouse Strains

Eight-week-old C57BL/6 mice were purchased from the National Cancer Institute (SAIC-Frederick, Inc., National Laboratory for Cancer Research, Frederick, MD), and MyD88 knockout (KO) animals (originally from Dr. Shizuo Akira, Osaka University, Osaka, Japan) were backcrossed >10 generations with C57BL/6 mice. Age- and sex-matched C57BL/6 mice were used as wild-type (WT) controls.

### Mouse Model of *S. aureus* Cranial Bone Flap Infection

A novel *S. aureus* cranial bone flap infection model was established by modifying a mouse cranial window procedure.<sup>10</sup> In brief, mice were anesthetized using avertin, and a cranial bone flap approximately 3 to 4 mm in diameter was made using a high-speed drill (Stryker Instruments, Kalamazoo, MI). After excision, the bone flap was immediately incubated in 500  $\mu$ L of a log-phase culture of the MRSA strain USA300 LAC (obtained from Dr. Frank DeLeo, National Institute of Allergy and Infectious Diseases Rocky Mountain Laboratories, Hamilton, MT)<sup>11</sup> in brain-heart infusion medium at 37°C for 5 minutes, and subsequently was rinsed with sterile PBS to remove any nonadherent bacteria. With this approach, bone flaps were initially evaluated using two infectious inoculums, namely, 10<sup>6</sup> or 10<sup>7</sup> colony forming units (CFU)/mL, which resulted in 10<sup>5</sup> and 10<sup>6</sup> CFU bacteria adherent to the bone, respectively. In control animals, bone flaps were excised using an identical procedure but were incubated in an equal volume of sterile brain-heart infusion medium before reinsertion into the cranium. The animal use protocol, approved by the University of Nebraska Medical Center Institutional Animal Care and Use Committee, was in accord with the NIH guidelines for the use of rodents.

### Neutrophil Depletion Studies

To evaluate the functional importance of neutrophils during the course of cranial bone flap infection, mice were transiently

depleted of neutrophils using a Gr-1 antibody as previously described.<sup>12</sup>

### Quantitation of Bacterial Titers

At designated intervals, bacterial burdens associated with the infected bone flap, an equivalently sized fragment of contralateral skull, approximately 1 mm of the superficial ipsilateral and contralateral cortex, and the ipsilateral galea were determined as previously described.<sup>13</sup>

### Flow Cytometry

To examine immune cell infiltration into the galea and brain parenchyma during bone flap infection, fluorescence-activated cell sorting (FACS) analysis was performed.<sup>13</sup> Cells were stained using Ly-6G, CD45, and F4/80 (BD Biosciences, San Diego, CA) to identify macrophages (CD45<sup>hi</sup> and F4/80<sup>+</sup>) and neutrophils (CD45<sup>hi</sup> and Ly-6G<sup>+</sup>). Cells were analyzed using a BD FACS LSR flow cytometer (BD Biosciences) with compensation set based on staining with each individual fluorochrome alone, and cells were incubated with isotype control antibodies to assess nonspecific staining. Analysis was performed using BD FACSDiva software version 6.2 (BD Biosciences) by gating on the total leukocyte (ie, CD45<sup>+</sup>) population.

### MILLIPLEX Multianalyte Microbead Array

To quantitate inflammatory mediator production during cranial bone flap infection, a MILLIPLEX microbead suspension array (EMD Millipore, Billerica, MA) was used, which detects CXCL1/KC, CXCL2/MIP-2, CXCL10/IP-10, CCL2/MCP-1, CCL5/RANTES, CCL9/MIG, IL-1 $\beta$ , IL-6, IL-9, IL-10, and IL-12 p70. Results were analyzed using a Bio-Plex Workstation (Bio-Rad Laboratories, Inc., Hercules, CA).

### Magnetic Resonance Imaging

After bone flap replacement, mice were evaluated at regular intervals via magnetic resonance imaging (MRI) to assess the degree of galeal inflammation and brain parenchymal involvement. Animals were anesthetized with 1.5% isoflurane in a 70% nitrous oxide/30% oxygen mixture and positioned in a custom-made stereotactic holder equipped with an MRI-compatible physiologic monitoring system (model 1025; SA Instruments, Inc., Stony Brook, NY). Core body temperature of anesthetized animals was maintained using a warm-air delivery system, and MRI data were obtained using an Advance 7-T 21-cm small-bore system (Bruker Corp., Madison, WI). Images were acquired using volume coil transmit, surface coil receive. T<sub>2</sub>-weighted images were acquired using rapid acquisition with refocused echoes (RARE), with TE 12 ms, RARE factor 8, effective TE 36 ms, TR 4200 ms, 20-mm field of view, 256  $\times$  256 acquisition matrix, 29 interleaved contiguous 0.5-mm thick sections, and total acquisition time of 3 minutes 21 seconds.

## Scanning Electron Microscopy

Mouse cranial bone flaps were fixed in 0.1 mol/L Sorensen's phosphate buffer containing 2.5% glutaraldehyde and 2% paraformaldehyde, and were subjected to critical point drying (Pelco CPD2; Ted Pella, Inc., Redding, CA). Bone flaps were mounted on aluminum stubs with carbon tabs and colloidal silver paste, sputter coated with gold-palladium (Hummer VI sputter coater; Anatech, Ltd., Battle Creek, MI), and viewed using a Quanta 200 scanning electron microscope (FEI Co., Hillsboro, OR) operated at 25 kV.

A cranial bone flap was obtained from a patient that developed a postoperative infection at 4 months. At hospital admission, a cerebrospinal fluid tap was performed, which confirmed *S. aureus* infection. After providing informed consent, the patient underwent surgery to remove the infected bone flap, and the discarded flap was processed for scanning electron microscopy (SEM). The bone flap was processed using the same procedure as described for mouse bone; however, rather than critical point drying, chemical drying was performed, which included incubations in 1:1 hexamethyldisilazane/100% ethyl alcohol followed by 100% hexamethyldisilazane for 30 minutes each.

## Statistical Analysis

Significant differences between treatment groups at a single time point were determined using a paired Student's *t*-test. Statistical analysis was performed using PRISM software version 4 (GraphPad Software, Inc., La Jolla, CA). *P* < 0.05 was considered statistically significant.

## Results

### Establishment of an *S. aureus* Cranial Bone Flap Infection Model

The first issue addressed when developing our model was identification of the optimal conditions for bone flap colonization. We elected to incubate autologous bone flaps with *S. aureus* before their replacement into the cranium because subcutaneous injection of bacteria would lead to abscess formation, which is rare in human skull flap infection. Bone flaps were removed via craniectomy and immediately incubated with *S. aureus* USA300 LAC at intervals ranging from 5 to 120 minutes using different bacterial inoculums (Supplemental Figure S1). Two inoculums, which resulted in colonization of  $10^5$  or  $10^6$  CFU *S. aureus* per bone flap, were selected for further analysis. All mice survived infection with both doses and exhibited typical sickness behavior during the first 24 hours, as evidenced by hunched posture, ruffled fur, and general malaise.

To define the chronicity of cranial bone flap infection and predilection of *S. aureus* for distinct anatomical regions, bacterial titers were determined up to 4 months after infection. Throughout the first month, bacterial burdens were highest on infected bone flaps compared with other regions, regardless of the infectious dose (Figure 1 and Supplemental Figure S2). Bacteria were also detected in the ipsilateral brain parenchyma; however, titers were lower than in bone (Figure 1). Similarly, bacteria were readily detected in the galea, the fascial layer between the skin and the calvaria, although no evidence of abscess formation was observed within the subcutaneous compartment over the 4-month infection period

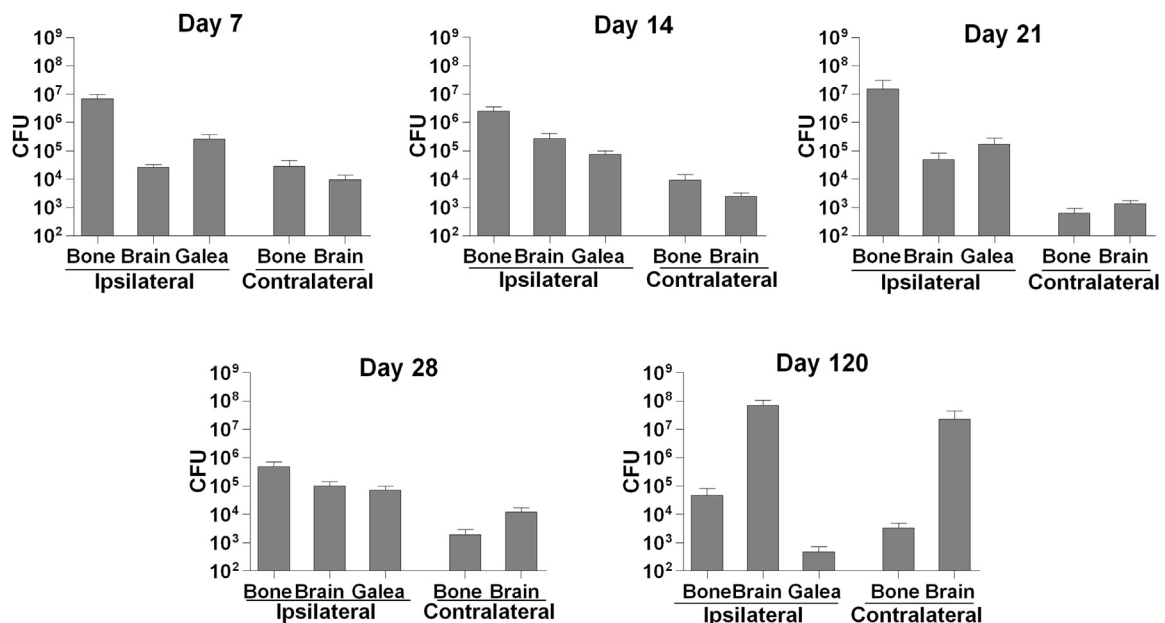
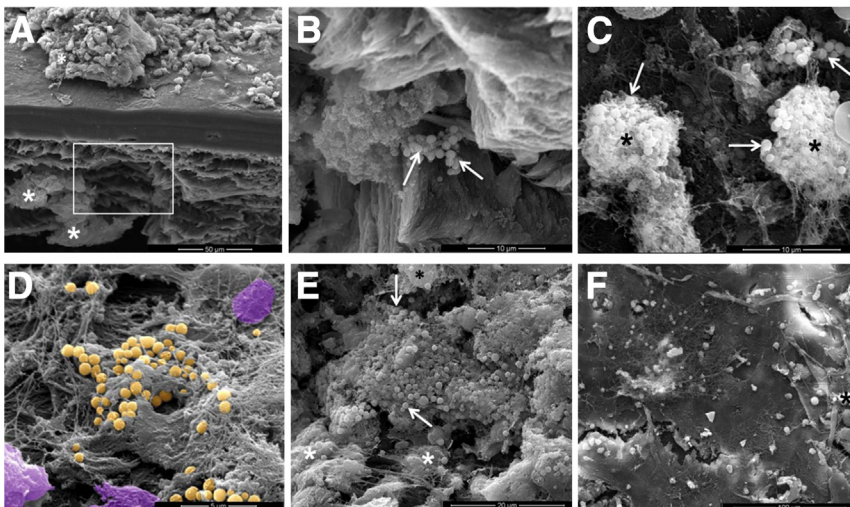


**Figure 1** *S. aureus* colonization of cranial bone flaps leads to persistent infection in multiple compartments. Infected bone flaps ( $10^5$  CFU) were reinserted after craniectomy. Mice were sacrificed at the indicated times after infection, and the numbers of viable bacteria on the ipsilateral bone flap, galea, and adjacent brain parenchyma were determined. Equivalent regions were also sampled from the contralateral hemisphere. Animals that received sterile bone flaps tested consistently negative for bacterial growth, and their data are not shown. Results are representative of combined data from 13 to 15 mice over the course of three independent experiments.

## Mouse Model



## Human

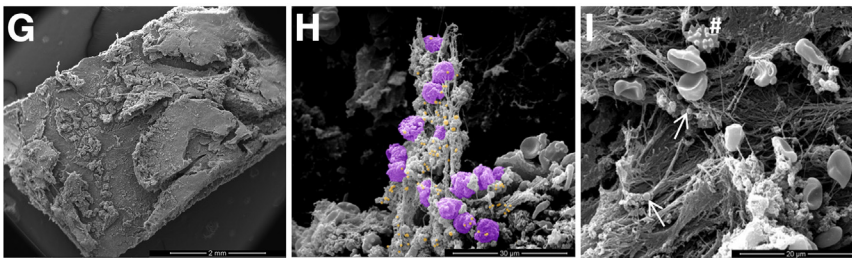


**Figure 2** *S. aureus* forms complex structures during cranial bone flap infection. SEM analysis of infected (A–E) and sterile (F) bone flaps from mice at day 7 after reinsertion into the cranium. **Inset** in A depicts the region magnified in B, highlighting a focus of *S. aureus* associated with the ventral bone flap surface. C: Cocoon-like structures harboring numerous bacteria. D and E: Various complex tertiary formations that were frequently observed on the bone flap surface. G–I: SEM images of a bone flap from a patient with confirmed *S. aureus* infection revealed similarities to the mouse model. G: Overview of the human bone flap surface reveals an irregular pattern of material deposition. H: Tertiary structure formed by interactions between leukocytes and *S. aureus*. I: Fiber deposition on the human bone flap surface shows remarkable similarity to the mouse model (D). Images in D and H have been pseudo-colored to highlight bacteria (gold) and leukocytes (purple). Bacteria are indicated by arrows, and host cells are depicted by either black or white asterisks. **Hash mark** in I indicates a crenated red blood cell artifact, which is also apparent in H. Scale bars: 50  $\mu\text{m}$  (A); 10  $\mu\text{m}$  (B and C); 5  $\mu\text{m}$  (D); 20  $\mu\text{m}$  (E and I); 100  $\mu\text{m}$  (F); 2 mm (G); and 30  $\mu\text{m}$  (H).

despite the presence of substantial exudate. The infection also extended to the contralateral skull and parenchyma (Figure 1 and Supplemental Figure S2); however, bacterial burdens in these regions progressively decreased over time, indicating a degree of infection containment. Of importance, mice subjected to craniectomy and replacement of autologous sterile bone flaps did not exhibit any evidence of bacterial growth on either the flap or other regions examined (data not shown).

Bacterial titers were generally higher in mice that received bone flaps colonized with  $10^6$  CFU compared with the lower dose of  $10^5$  CFU in all regions examined (Figure 1 and Supplemental Figure S2). A heightened inflammatory response in animals that received bone flaps colonized with  $10^6$  CFU was apparent in that some mice exhibited wound breakdown and bone flap loss by day 10, potentially from eschar extrusion or autolysis. In contrast, animals that received bone flaps colonized with  $10^5$  CFU did not demonstrate any evidence of eschar formation, and flaps remained infected up to 120 days after insertion (Figure 1), confirming the chronicity of infection in our model. On the basis of these findings, all subsequent experiments used the lower infectious inoculum (ie,  $10^5$  CFU).

Demonstration of Bone Flap Colonization *in Vivo*

To verify *S. aureus* persistence on bone flaps *in vivo*, SEM imaging was performed. The most striking observation was robust leukocyte accumulation on both surfaces of infected bone flaps (Figure 2A). Bacteria were typically clustered in

areas where leukocyte infiltrates were observed, and appeared either as large solitary aggregates (Figure 2, B–D), directly interacting with the leukocyte surface (Figure 2, C and E), or as single organisms encased in a fibrous network (Figure 2D). Fiber deposition was also observed on the surface of sterile bone flaps (Figure 2F), which suggested that a portion of this response was host-derived. Leukocytes were also associated with sterile bone flaps (Figure 2F); however, their numbers were dramatically reduced compared to infected bone.

SEM images of a bone flap from a patient with confirmed *S. aureus* infection revealed structural similarities to the mouse model. An overview of the human bone flap surface (Figure 2G) revealed an irregular pattern of material deposition, with extensive tertiary structures formed by interactions between leukocytes and *S. aureus* (Figure 2H). In addition, fiber deposition on the human bone flap surface (Figure 2I) revealed remarkable similarity to the mouse model (Figure 2D). The irregularity of bacterial colonization on the human bone flap surface, presence of numerous leukocyte infiltrates, formation of secondary/tertiary structures composed of both leukocytes and bacteria, and deposition of extensive fibrous matrix on the bone surface demonstrated that our mouse model displayed good structural fidelity to human cranial bone flap infection.

## MRI Analysis Reveals Similarities between the Mouse Cranial Bone Flap Infection Model and Human Disease

MRI is the primary method used to diagnose human bone flap infections,<sup>8,14</sup> most of which are typified by robust

subgaleal inflammation and limited parenchymal involvement.<sup>15,16</sup> MRI analysis revealed prominent inflammation in the galea until day 14 after infection, with minimal parenchymal involvement (Figure 3). Placement of sterile bone flaps showed little evidence of inflammatory changes and completely coalesced with the surrounding skull by day 21 after cranioplasty (Figure 3). Histologic examination at day 7 confirmed lack of substantial cortical involvement in mice that received flaps with the lower dose inoculum compared with sterile bone (Supplemental Figure S3).

### Compartmentalization of Inflammatory Indices during *S. aureus* Cranial Bone Flap Infection

Gross examination of the ipsilateral galea and underlying cortex associated with infected bone flaps suggested that the degree of inflammation differed in both compartments. Specifically, exudate was clearly visible in the galea, whereas the adjacent brain parenchyma showed no gross evidence of exudate, edema, or abscess formation. Despite the presence of bacteria in the ipsilateral brain parenchyma, neutrophil infiltrates were minimal during the acute phase of infection (ie, days 7 to 14) (Figure 4A). In contrast, neutrophil influx was markedly elevated in the galea at the same intervals (Figure 4A). This was intriguing because the absolute numbers of bacteria were not dramatically different in both regions (Figure 1) and bone flaps were colonized on both surfaces, as demonstrated by SEM analysis (Figure 2A). Regarding macrophage accumulation, the opposite relationship was observed. Specifically, there were no differences in macrophage infiltrates during acute infection (ie, day 7); however, after this interval, macrophages were increased in the ipsilateral brain parenchyma compared with the galea,

where the number of macrophages progressively declined (Figure 4B).

We next examined whether the observed differences in leukocyte influx correlated with altered chemokine expression patterns in the ipsilateral galea and cortex. CXCL2 and CCL5, potent neutrophil and monocyte/T-cell chemokines, respectively, were prominent in the galea, whereas expression was minimal in the ipsilateral cortex (Figure 5). In contrast, the T-cell chemokine CXCL10<sup>17,18</sup> was primarily detected in the parenchymal compartment (Figure 5), which was interesting because T-cell infiltrates (ie, CD3<sup>+</sup>) were low or undetectable throughout the course of infection (data not shown). Collectively, these results demonstrate the existence of two microenvironments that respond uniquely to *S. aureus* despite being exposed to equivalent numbers of bacteria on both bone flap surfaces.

### MyD88-Dependent Signals Regulate Early Bacterial Containment and Inflammatory Mediator Expression during *S. aureus* Cranial Bone Flap Infection

We next used MyD88 KO mice to examine whether this adaptor was critical for eliciting proinflammatory responses during cranial bone flap infection. MyD88 is a key adaptor molecule required for signaling through most Toll-like receptors, as well as IL-1R, IL-18R, and IL-33R,<sup>19,20</sup> and numerous studies have demonstrated a critical role for MyD88 in host immunity to staphylococcal infections including brain abscesses, pneumonia, and dermal infections.<sup>21–23</sup> MyD88 KO animals became moribund by day 2 after infection, and premature euthanasia was necessary to prevent survival bias. This revealed a critical role for MyD88 because WT animals rarely succumbed to infection. Compared with WT animals, bacterial

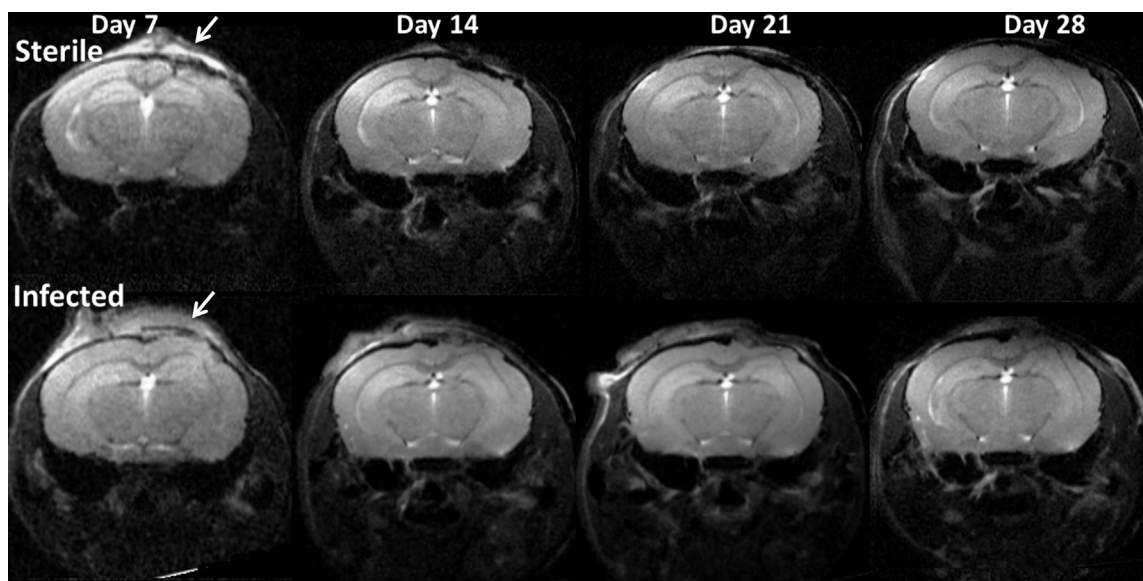


**Figure 3** MRI analysis reveals prominent galeal inflammation during *S. aureus* cranial bone flap infection. Sterile or infected ( $10^5$  CFU) bone flaps were reinserted after craniectomy, and mice were subjected to MRI analysis at weekly intervals to day 28 after flap reinsertion into the cranium. **Arrows** indicate the region of bone flap replacement in T2-weighted RARE images from the same mouse over time. Results are representative of eight individual mice per group.

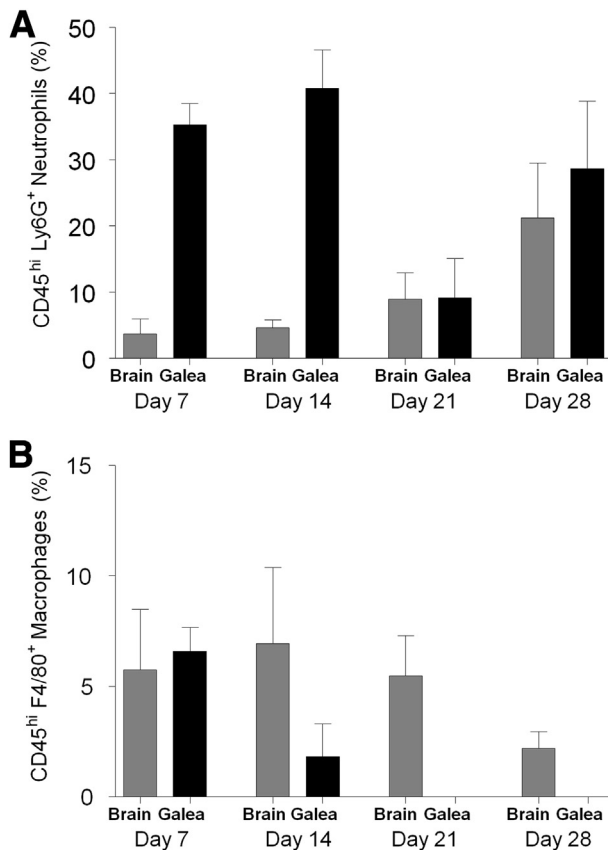


**Figure 4** Differential recruitment of neutrophils and macrophages into distinct compartments during cranial bone flap infection. Infected bone flaps ( $10^5$  CFU) were reinserted after craniectomy. Mice were sacrificed at weekly intervals extending to day 28 after infection, and percentages of neutrophils (A) and macrophages (B) infiltrating the ipsilateral galea and adjacent brain parenchyma were determined by FACS. Results were combined from three independent experiments.

burdens in MyD88 KO mice were significantly elevated ( $P < 0.05$ ) in all ipsilateral and contralateral regions examined, indicating that MyD88-dependent signals are required for bacterial containment during acute infection (Figure 6A). In addition, the influx of CD45<sup>+</sup> leukocytes and neutrophils was reduced in MyD88 KO mice (Figure 6B), which likely contributed to the observed defect in bacterial containment. Although raw cytokine/chemokine values revealed minimal differences between MyD88 KO and WT animals, normalization to account for elevated bacterial burdens in the former resulted in reduced expression of IL-1 $\beta$ , CXCL1, and other mediators in MyD88 KO mice (Figure 6, C and D) ( $P < 0.05$  and data not shown). However, there was also evidence for MyD88-independent pathways driving inflammation because residual cytokine/chemokine expression was still detected in MyD88 KO mice (Figure 6, C and D, and data not shown).

### Neutrophils Are Critical Effectors during Acute *S. aureus* Cranial Bone Flap Infection

Neutrophils are crucial antimicrobial phagocytes that possess an arsenal of effector molecules including proteases, reactive

oxygen species, antimicrobial peptides, and neutrophil extracellular traps.<sup>24,25</sup> Because neutrophil infiltrates predominated in the galea throughout the course of cranial bone flap infection, their functional importance was assessed. Mice subjected to antibody-mediated depletion of neutrophils displayed a moribund phenotype similar to that in MyD88 KO animals, which required premature euthanasia at day 2 after infection to prevent survival bias. Accordingly, bacterial burdens were significantly elevated ( $P < 0.05$ ) on both the ipsilateral bone flap and the galea after neutrophil depletion (Figure 7A). Although there were no differences in absolute cytokine/chemokine levels between neutrophil-depleted and control mice, adjustment of values to account for elevated bacterial burdens in the former resulted in significant decreases ( $P < 0.05$ ) in CXCL2, IL-1 $\beta$ , and CXCL10 in neutrophil-depleted mice (Figure 7, B–D), reminiscent of results obtained in MyD88 KO animals (Figure 6). Therefore, although neutrophils are not effective in clearing *S. aureus* bone flap infection in this model, as evidenced by persistent colonization, in the early phase of infection they are important for containing bacterial burdens and induction of specific inflammatory mediators.

Collectively, these findings indicate that bacterial containment and inflammatory mediator release during the early phase of *S. aureus* cranial bone flap infection are partially neutrophil- and MyD88-dependent. Because both neutrophil-depleted and MyD88 KO mice became moribund by day 2 after infection, the differences in immune compartmentalization described at day 7 (Figures 4 and 5) were not yet apparent.

## Discussion

Bone flap infection is a serious complication of decompressive craniectomy that requires additional surgical procedures and has important economic consequences. The cellular and molecular events during cranial bone flap infection are not well characterized, and immune responses to this infection remain largely unexplored. This is the first report, to our knowledge, that sought to replicate cranial bone flap infection by establishing a mouse model that exhibits both clinical and radiologic features similar to those of human disease.

One intriguing observation that emerged in the present study was differential compartmentalization of proinflammatory responses and leukocyte infiltrates in the galea versus the brain parenchyma. For example, monocyte chemokines (ie, CCL2 and CCL5) were markedly elevated in the galea throughout infection, yet macrophage infiltrates were observed in this compartment only during the early stage. Similarly, neutrophil influx was equivalent in the galea and parenchyma at days 21 and 28 after infection, yet CXCL2 was more prominent in the galea. Collectively, these findings imply the action of additional chemokines. Alternatively, neutrophil accumulation during late-stage infection could be triggered by the inability of resident glia and/or regional macrophage populations to contain the infection. Indeed, animals that received the low dose inoculum displayed well-demarcated exudate in the subcutaneous galea at 4 months after infection and on removal

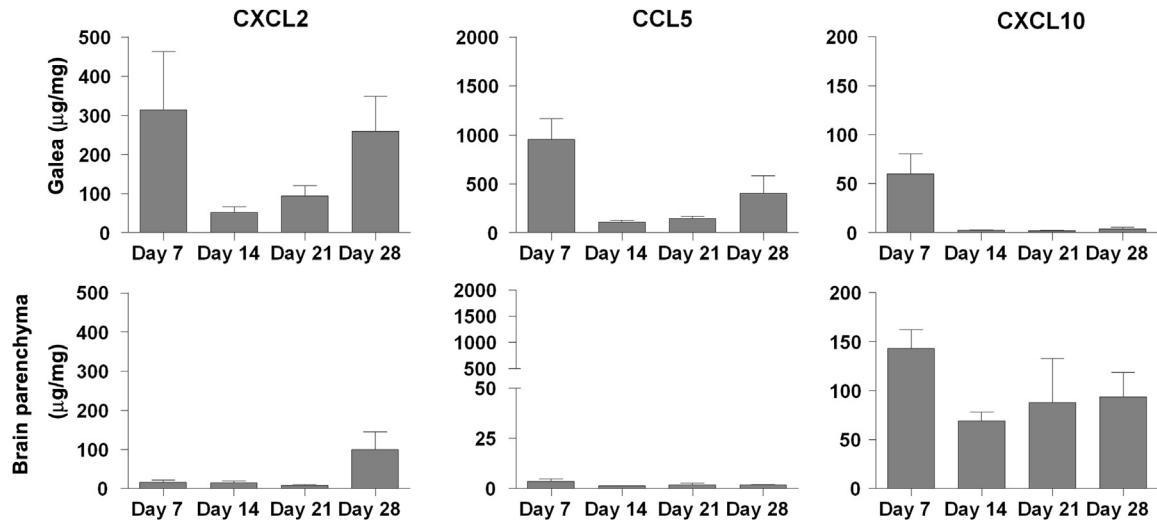


**Figure 5** Chemokines are preferentially expressed in distinct compartments during *S. aureus* cranial bone flap infection. Infected bone flaps ( $10^5$  CFU) were reinserted after craniectomy. Mice were sacrificed at weekly intervals extending to day 28 after infection, and CXCL2, CCL5, and CXCL10 expression in the ipsilateral galea and adjacent brain parenchyma was determined using multianalyte bead arrays. Results are normalized to the amount of total protein to correct for differences in tissue sampling size.

of the skull, substantial erosion of the superficial cortex along with well-circumscribed exudate (Supplemental Figure S3). Another explanation for why inflammatory responses were more robust in the galea than in the central nervous system parenchyma despite nearly equivalent bacterial burdens is that the galea is not restricted by the blood-brain barrier. In addition, infected bone flaps are separated from the brain parenchyma by the meninges, which may account for the minimal inflammation observed in this compartment. Bacterial persistence within the galea was also intriguing because delayed bone flap replacement is common practice in the clinical setting due to the high incidence of reinfection despite antibiotic therapy.<sup>26,27</sup> On the basis of these findings, the galea may represent a reservoir for infection persistence; however, this possibility remains to be verified with clinical samples.

Ultrastructural analysis of infected bone flaps revealed an extensive meshlike network on both surfaces. Because fiber deposition was also associated with sterile bone flaps, a portion of this response is host-derived and likely enhances bacterial attachment. This fibrous network was substantially more extensive in the context of infection, indicating an active role of bacteria in eliciting this response. Although it is attractive to consider that some of the tertiary structures visualized on bone flaps by SEM represent biofilm formation, additional studies are needed to verify this possibility. Another interesting observation was that numerous bacteria were encased in structures that appeared cocoon-like. These formations were primarily associated with the dorsal aspects of infected bone flaps and coincided with regions where substantial leukocyte accumulation was evident. We propose

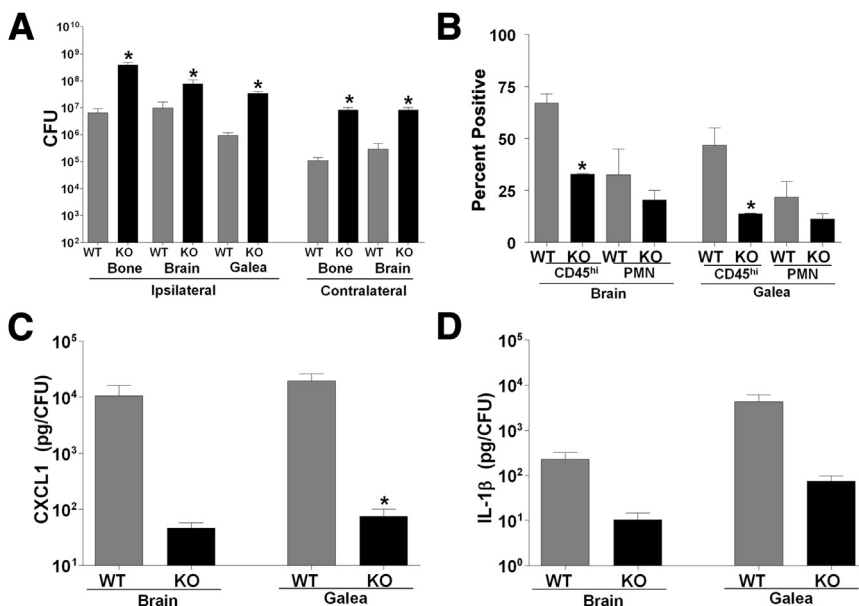


**Figure 6** MyD88-dependent signaling is important for bacterial containment and proinflammatory mediator secretion during *S. aureus* cranial bone flap infection. Infected bone flaps ( $10^5$  CFU) were reinserted in MyD88 KO and WT mice after craniectomy. Animals were sacrificed at day 2 after infection, and bacterial burdens (A), CD45<sup>+</sup> leukocyte and neutrophil (PMN) infiltrates (B), and CXCL1 (C) and IL-1β (D) expression associated with the ipsilateral galea and adjacent brain parenchyma were evaluated. CXCL1 and IL-1β levels were determined using multianalyte bead arrays and are normalized to bacterial burdens. Results are representative of two independent experiments. \* $P < 0.05$ .

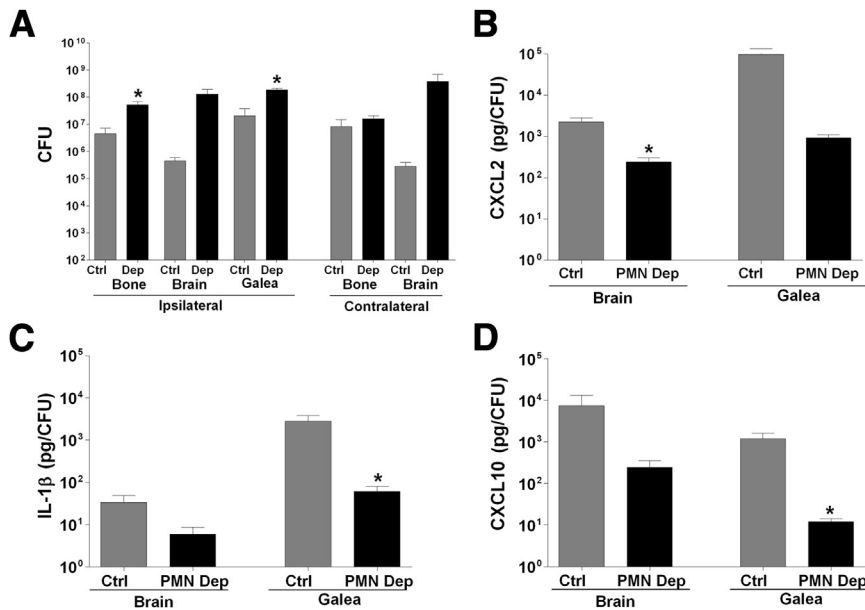


**Figure 7** Neutrophils are critical for controlling bacterial burdens and eliciting proinflammatory mediator expression during cranial bone flap infection. Infected bone flaps ( $10^5$  CFU) were reinserted in neutrophil-depleted (PMN Dep) and control (Ctrl) mice after craniectomy. Animals were sacrificed at day 2 after infection, and bacterial burdens (A) and CXCL2 (B), IL-1 $\beta$  (C), and CXCL10 (D) expression associated with the ipsilateral galea and adjacent brain parenchyma were evaluated. CXCL2, IL-1 $\beta$ , and CXCL10 levels were determined using multi-analyte bead arrays and are normalized to bacterial burdens. Results are representative of two independent experiments. \* $P < 0.05$ .

that these structures may represent neutrophil and/or macrophage extracellular traps, which are composed of mammalian DNA and decorated with islands of degradative enzymes thought to kill bacteria after neutrophil/macrophage death has occurred,<sup>28,29</sup> although this possibility remains speculative.

Several intriguing comparisons can be made between our *S. aureus* cranial bone flap infection model and previous studies of *S. aureus* brain abscess and peripheral biofilm infection.<sup>13,30–32</sup> First, compared with the bone flap model, brain abscesses elicit substantially more parenchymal inflammation, focal tissue destruction, and edema.<sup>13,21,32</sup> However, brain abscesses resolve within approximately 14 to 21 days, which was not observed in the cranial bone flap model despite using similar infectious doses. This suggests that the bone flap serves as a foreign body to facilitate bacterial persistence, which is reinforced by the finding that infection was still detected up to 4 months, the latest interval examined to date. Second, a similar requirement for MyD88-dependent signals in inducing inflammatory mediator production was shown for both the *S. aureus* cranial bone flap and brain abscess models.<sup>21</sup> In contrast, MyD88 only was critical for regulating bacterial burdens during cranial bone flap infection, whereas titers between MyD88 KO and WT mice in the brain abscess model were similar.<sup>21</sup> Third, similar phenotypes were observed during *S. aureus* cranial bone flap and catheter-associated biofilm infection in the periphery in MyD88 KO mice, in which bacterial titers were elevated and expression of selected inflammatory mediators was repressed.<sup>31</sup> Collectively, these findings highlight the disparities between the requirement for MyD88 signaling in eliciting proinflammatory mediators and bacterial containment during *S. aureus* infection, which is likely influenced by the anatomical location and type of infection (ie, soft tissue versus bone or catheter).

We have previously reported that structurally mature biofilms elicit an anti-inflammatory, profibrotic response

dominated by M2 macrophage accumulation.<sup>30</sup> Macrophage infiltrates were not phenotyped as M1/M2 in these studies; however, it is evident by the pronounced proinflammatory mediator expression and neutrophil influx in the galea that infected bone flaps elicit a distinct immune profile from that observed during biofilm infection. Nonetheless, it is clear that this response is ineffective because *S. aureus* persists, which is in agreement with our concept that chronic *S. aureus* infections evade traditional microbicidal responses.<sup>33</sup>

Although we recognize that preadherence of *S. aureus* to excised skull flaps does not mimic native colonization in humans, this approach was required because direct subcutaneous injection of bacteria would have led to abscess formation, which is distinct from the clinical features of cranial bone flap infections in humans. Of importance, SEM analysis of a cranial bone flap from a patient with confirmed *S. aureus* infection demonstrated similar structural characteristics as our mouse model, including the irregular nature of bacterial colonization on the bone surface, presence of numerous leukocyte infiltrates, formation of secondary/tertiary structures composed of both leukocytes and bacteria, and deposition of an extensive fibrous matrix on the bone surface. These findings, coupled with our MRI analysis showing that our mouse model exhibits good radiologic fidelity to human cranial bone flap infection, suggest that our method of bone flap infection elicits a response that closely parallels numerous facets of human disease.

In conclusion, cranial bone flap infection is a frequent complication after decompressive craniectomy despite modern aseptic technique. The clinical sequelae of bone flap infection necessitate multiple surgical procedures and include the potential for clinical deterioration and need for costly custom implants. The model described here will enable future investigations to elucidate both host- and bacteria-derived factors that shape the development of chronic cranial bone flap infections.

## Acknowledgments

We thank Dr. David Muirhead and Melissa Holzapfel for assistance with SEM analysis, Dr. Charles Kuszynski and Victoria Smith [University of Nebraska Medical Center (UNMC) Cell Analysis Facility] for support with FACS analysis, Amanda Angle for technical assistance, Melissa Mellon (UNMC Small Animal Imaging Core Facility) for assistance with MRI analysis, the UNMC Tissue Sciences Facility for imaging of H&E-stained tissues, Drs. Jessica Snowden and Mark Hanke for critical review of the manuscript, and Dr. Hanke for assistance with the figures.

## Supplemental Data

Supplemental material for this article can be found at <http://dx.doi.org/10.1016/j.ajpath.2013.04.031>.

## References

- Bhaskar IP, Zaw NN, Zheng M, Lee GY: Bone flap storage following craniectomy: a survey of practices in major Australian neurosurgical centres. *ANZ J Surg* 2011, 81:137–141
- Dashti SR, Baharvahdat H, Spetzler RF, Sauvageau E, Chang SW, Stiefel MF, Park MS, Bambakidis NC: Operative intracranial infection following craniotomy. *Neurosurg Focus* 2008, 24:E10
- Baumeister S, Peek A, Friedman A, Levin LS, Marcus JR: Management of postneurosurgical bone flap loss caused by infection. *Plast Reconstr Surg* 2008, 122:195e–208e
- Hammon WM, Kempe LG: Methyl methacrylate cranioplasty: 13 years experience with 417 patients. *Acta Neurochir (Wien)* 1971, 25:69–77
- Honeybul S, Ho KM: Long-term complications of decompressive craniectomy for head injury. *J Neurotrauma* 2011, 28:929–935
- Fodstad H, Love JA, Ekstedt J, Fridén H, Liliequist B: Effect of cranioplasty on cerebrospinal fluid hydrodynamics in patients with the syndrome of the trephined. *Acta Neurochir (Wien)* 1984, 70:21–30
- Grant FC, Norcross NC: Repair of cranial defects by cranioplasty. *Ann Surg* 1939, 110:488–512
- Sinclair AG, Scoffings DJ: Imaging of the post-operative cranium. *Radiographics* 2010, 30:461–482
- Yang XF, Wen L, Shen F, Li G, Lou R, Liu WG, Zhan RY: Surgical complications secondary to decompressive craniectomy in patients with a head injury: a series of 108 consecutive cases. *Acta Neurochir (Wien)* 2008, 150:1241–1247. discussion 1248
- Yang G, Pan F, Parkhurst CN, Grutzendler J, Gan WB: Thinned-skull cranial window technique for long-term imaging of the cortex in live mice. *Nat Protoc* 2010, 5:201–208
- Kennedy AD, Otto M, Braughton KR, Whitney AR, Chen L, Mathema B, Mediavilla JR, Byrne KA, Parkins LD, Tenover FC, Kreiswirth BN, Musser JM, DeLeo FR: Epidemic community-associated methicillin-resistant *Staphylococcus aureus*: recent clonal expansion and diversification. *Proc Natl Acad Sci U S A* 2008, 105:1327–1332
- Kielian T, Barry B, Hickey WF: CXC chemokine receptor-2 ligands are required for neutrophil-mediated host defense in experimental brain abscesses. *J Immunol* 2001, 166:4634–4643
- Aldrich A, Kielian T: Central nervous system fibrosis is associated with fibrocyte-like infiltrates. *Am J Pathol* 2011, 179:2952–2962
- Blumenkopf B, Hartshorne MF, Bauman JM, Cawthon MA, Patton JA, Friedman AH: Craniotomy flap osteomyelitis: a diagnostic approach. *J Neurosurg* 1987, 66:96–101
- Pandey AS, Surana A: Tuberculous osteomyelitis of the bone flap following craniotomy. *Indian J Tuberc* 2011, 58:129–131
- Dujovny M, Fernandez P, Alperin N, Betz W, Misra M, Mafee M: Post-cranioplasty cerebrospinal fluid hydrodynamic changes: magnetic resonance imaging quantitative analysis. *Neurol Res* 1997, 19:311–316
- Valbuena G, Bradford W, Walker DH: Expression analysis of the T-cell-targeting chemokines CXCL9 and CXCL10 in mice and humans with endothelial infections caused by rickettsiae of the spotted fever group. *Am Pathol* 2003, 163:1357–1369
- Norose K, Kikumura A, Luster AD, Hunter CA, Harris TH: CXCL10 is required to maintain T-cell populations and to control parasite replication during chronic ocular toxoplasmosis. *Invest Ophthalmol Vis Sci* 2011, 52:389–398
- Ho LH, Ohno T, Oboki K, Kajiwara N, Suto H, Iikura M, Okayama Y, Akira S, Saito H, Galli SJ, Nakae S: IL-33 induces IL-13 production by mouse mast cells independently of IgE-FcεpsilonRI signals. *J Leukoc Biol* 2007, 82:1481–1490
- Wang JP, Lee CK, Akalin A, Finberg RW, Levitz SM: Contributions of the MyD88-dependent receptors IL-18R, IL-1R, and TLR9 to host defenses following pulmonary challenge with *Cryptococcus neoformans*. *PLoS One* 2011, 6:e26232
- Kielian T, Phulwani NK, Esen N, Syed MM, Haney AC, McCastlain K, Johnson J: MyD88-dependent signals are essential for the host immune response in experimental brain abscess. *J Immunol* 2007, 178:4528–4537
- Bello-Irizarry SN, Wang J, Olsen K, Gigliotti F, Wright TW: The alveolar epithelial cell chemokine response to pneumocystis requires adaptor molecule MyD88 and interleukin-1 receptor but not toll-like receptor 2 or 4. *Infect Immun* 2012, 80:3912–3920
- Makino M, Uemura N, Moroda M, Kikumura A, Piao LX, Mohamed RM, Aosai F: Innate immunity in DNA vaccine with *Toxoplasma gondii*-heat shock protein 70 gene that induces DC activation and Th1 polarization. *Vaccine* 2011, 29:1899–1905
- Amulic B, Cazalet C, Hayes GL, Metzler KD, Zychlinsky A: Neutrophil function: from mechanisms to disease. *Annu Rev Immunol* 2012, 30:459–489
- von Kockritz-Blickwede M, Nizet V: Innate immunity turned inside-out: antimicrobial defense by phagocyte extracellular traps. *J Mol Med (Berl)* 2009, 87:775–783
- Chiang HY, Steelman VM, Pottinger JM, Schlueter AJ, Diekema DJ, Greenlee JD, Howard MA 3rd, Herwaldt LA: Clinical significance of positive cranial bone flap cultures and associated risk of surgical site infection after craniotomies or craniectomies. *J Neurosurg* 2011, 114:1746–1754
- Vilela MD: Delayed paradoxical herniation after a decompressive craniectomy: case report. *Surg Neurol* 2008, 69:293–296. discussion 296
- Pilszczek FH, Salina D, Poon KK, Fahey C, Yipp BG, Sibley CD, Robbins SM, Green FH, Surette MG, Sugai M, Bowden MG, Hussain M, Zhang K, Kubes P: A novel mechanism of rapid nuclear neutrophil extracellular trap formation in response to *Staphylococcus aureus*. *J Immunol* 2010, 185:7413–7425
- Young RL, Malcolm KC, Kret JE, Caceres SM, Poch KR, Nichols DP, Taylor-Cousar JL, Saavedra MT, Randell SH, Vasil ML, Burns JL, Moskowitz SM, Nick JA: Neutrophil extracellular trap (NET)-mediated killing of *Pseudomonas aeruginosa*: evidence of acquired resistance within the CF airway, independent of CFTR. *PLoS One* 2011, 6:e23637
- Thurlow LR, Hanke ML, Fritz T, Angle A, Aldrich A, Williams SH, Engebretsen IL, Bayles KW, Horswill AR, Kielian T: *Staphylococcus aureus* biofilms prevent macrophage phagocytosis and attenuate inflammation in vivo. *J Immunol* 2011, 186:6585–6596
- Hanke ML, Angle A, Kielian T: MyD88-dependent signaling influences fibrosis and alternative macrophage activation during *Staphylococcus aureus* biofilm infection. *PLoS One* 2012, 7:e42476
- Nichols JR, Aldrich AL, Mariani MM, Vidlak D, Esen N, Kielian T: TLR2 deficiency leads to increased Th17 infiltrates in experimental brain abscesses. *J Immunol* 2009, 182:7119–7130
- Hanke ML, Kielian T: Deciphering mechanisms of staphylococcal biofilm evasion of host immunity. *Front Cell Infect Microbiol* 2012, 2:62